



$\frac{\partial \psi}{\partial t} + \frac{M}{2} \frac{|u(x,t)|^2}{\rho} + \frac{\Delta \psi}{\rho} + \frac{\Delta p}{\rho} = 0, \quad \nabla \psi \cdot \frac{\partial \psi}{\partial t} = u_0(x), \quad \psi(x,t) = e^{-\dots}$

# Azimuthal variations of X-band medium grazing angle sea clutter

Z. Guerraou<sup>(1)</sup>, S. Angelliaume<sup>(1)</sup>, C.-A. Guérin<sup>(2)</sup> and L. Rosenberg<sup>(3)</sup>

- (1) : ONERA, the French Aerospace Lab – France
- (2) : University of Toulon, MIO laboratory – France
- (3) : Defence Science and Technology Groupe - Australia



# ONERA ACTIVITIES – Sea surface radar imagery

## Improving our knowledge of the EM scattered signal from the sea surface

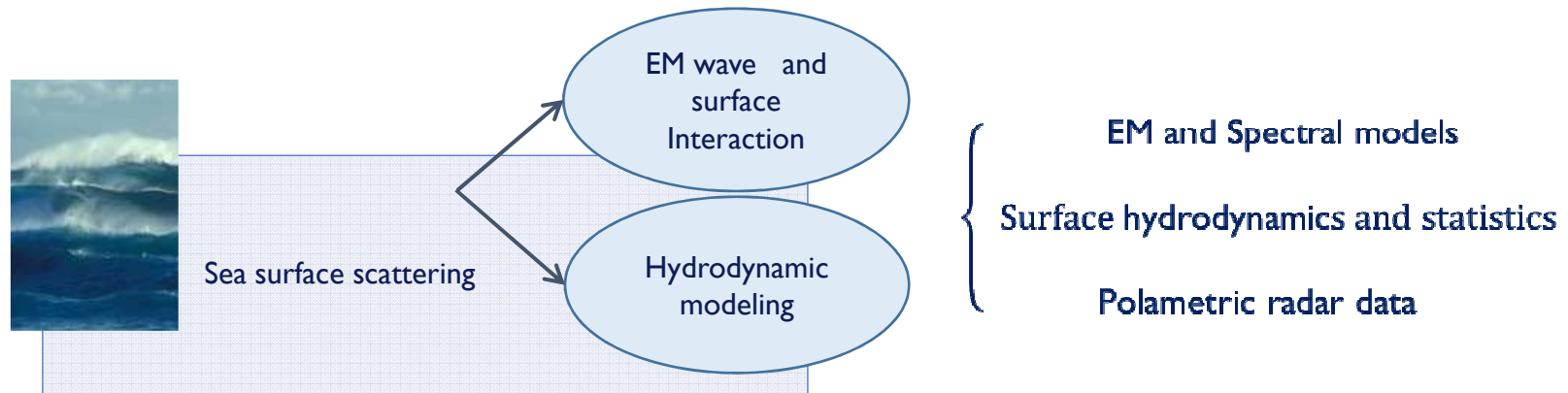
- Target detection: Developing robust detection methods under difficult sea conditions (Detection of small targets, rough sea state...)
- EM modeling of the sea clutter
- Detection/ characterization/ quantification of marine pollutants. (POLLUPROOOF project)
- Inversion of ocean surface parameters (wind/ wave heights/ ocean currents...)

## Collaborative work:

- ONERA – Research labs (MIO, DSTO ...)
- ONERA – Industrial organizations (TOTAL)



# CONTEXT OF THE STUDY



## Various challenges :

- Modeling of the HH and HV returns
- The variability of the NRCS
- The directional wave number spectrum of the short waves
- Azimuthal variations and directional asymmetries
- Breaking waves, sea spikes
- Grazing angle configuration...

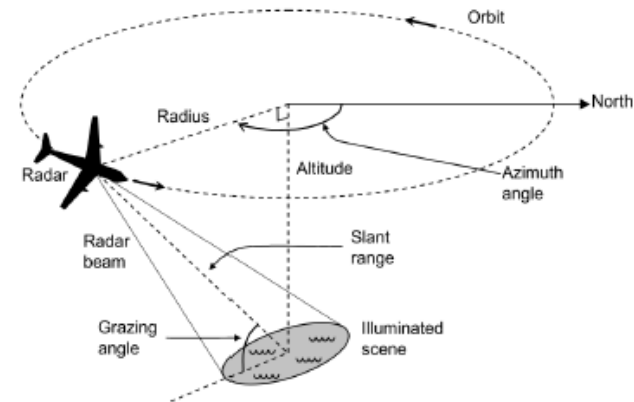
## The purpose:

Recent progresses toward the depiction and simulation of some of these phenomena.

# INGARA SYSTEM

Fully-polarimetric X band radar system maintained & operated within the « **D**efence **S**cience & **T**echnology **O**rganisation »

Frequency	10.1 GHz
Grazing angles	15° à 45°
Range resolution	0.75 m
Cross-range resolution	62 m



*INGARA radar and trial parameters (reproduced from [1])*

*Circular spotlight mode collection for the INGARA data (reproduced from [1])*

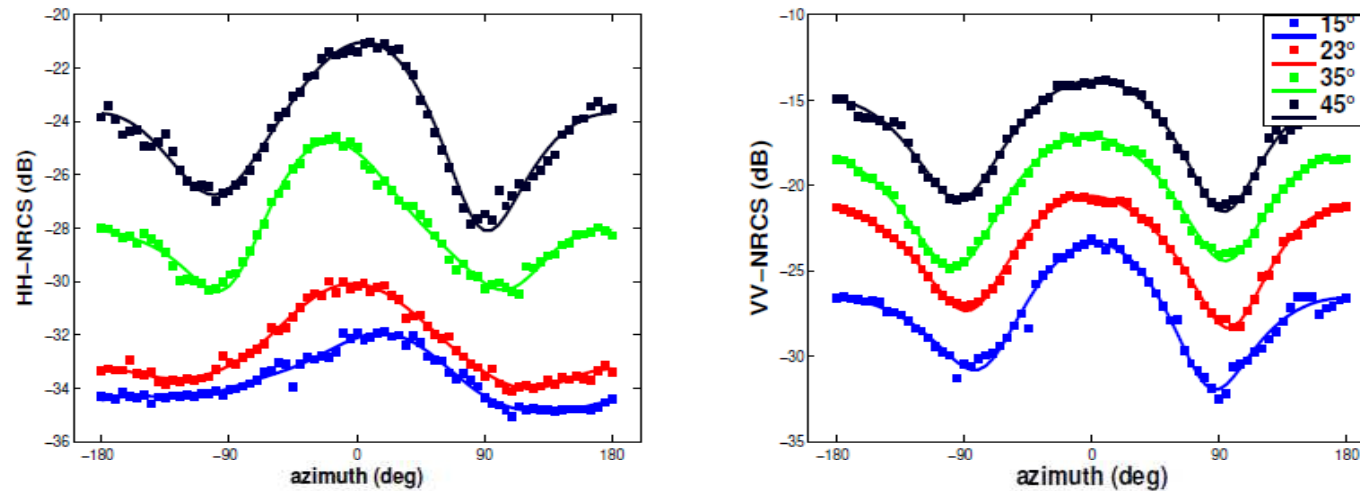
Trial	Flight	Date	Wind		Wave		
			Speed (m/s)	Direction (deg)	Height (m)	Direction (deg)	Period (s)
SCT04	F33	9/8/04	10.2	248	4.9	220	12.3
SCT04	F34	10/8/04	7.9	248	3.5	205	11.8
SCT04	F35	11/8/04	10.3	315	2.6	210	10.4
SCT04	F36	12/8/04	13.6	0	3.2	293	8.8
SCT04	F37	16/8/04	9.3	68	2.5	169	9.7
SCT04	F39	20/8/04	9.5	315	3.0	234	11.4
SCT04	F40	24/8/04	13.2	22	3.8	254	12.2
SCT04	F42	27/8/04	8.5	0	4.3	243	12.5
MAST06	F2	17/5/06	8.5	115	0.62	112	3.1
MAST06	F4	19/5/06	3.6	66	0.25	35	2.6
MAST06	F8	23/5/06	3.5	83	0.41	46	4.0
MAST06	F9	24/5/06	10.2	124	1.21	128	4.6

*Wind and wave ground truth for the Ingara data (reproduced from [1])*

[1] Crisp, D.J., R. Kyprianou, L. Rosenberg, and N.J. Stacy, *Modelling the mean ocean backscatter coefficient in the plateau region at X-band*. Research report, DSTO, 2012.



# Experimental observation: azimuthal variation of the NRCS



A vanishing of the secondary downwind maximum is observed with the HH pol at lowest grazing angle (as modelled in the empirical GIT mean backscattered model). This directional asymmetries are shown to be polarization-dependant and follow non-monotonic variations with respect to the grazing angle.

For the lower grazing angle, the SNR (particularly at HH pol) is low and an accurate denoising procedure is of primary importance to correct retrieval of the NRCS

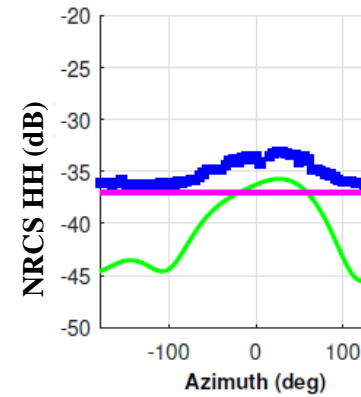
# Azimuthal variation of the NRCS : *Maximum Likelihood estimation*

$$\sigma_0^{model}(\phi_n) = \tilde{\sigma}_0(\phi_n) + b(\phi_n)$$

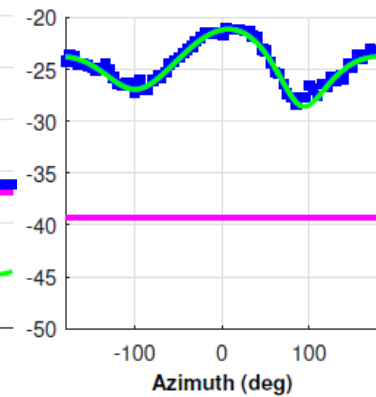
**Model:** Truncated Fourier series

$$\tilde{\sigma}_0(\phi_n) = a_0 + \sum_{k=1}^4 a_k \cos(k(\phi_n - \delta_k))$$

Grazing: 15°



45°



Raw NRCS  
Mean noise estimate  
Denoised NRCS

Upwind = 0°  
Downwind = +/- 180°  
Crosswind = +/- 90°

**Log-Likelihood:**

$$\mathcal{L} = -\frac{1}{2} \sum_{n=1}^{N_a} \log(2\pi\sigma_0^2) - \sum_{n=1}^{N_a} \frac{1}{2\sigma_0^2} [\sigma_0^{data}(\phi_n) - (\tilde{\sigma}_0(\phi_n) + \bar{b})]^2$$

$$\frac{\partial \mathcal{L}}{\partial a_k} = 0, \quad \frac{\partial \mathcal{L}}{\partial \phi_k} = 0 \dots \longrightarrow a_n, \phi_n$$

# Angular variation of the denoised NRCS: grazing variations

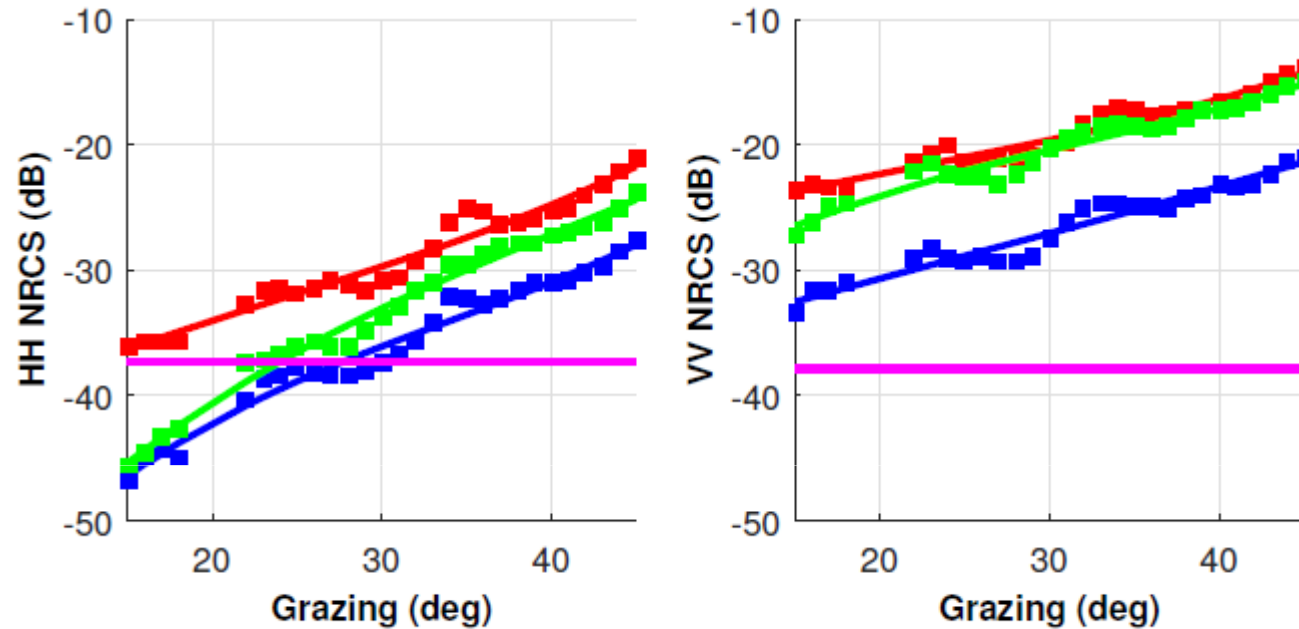
Run day 9

Upwind

Crosswind

Downwind

Noise floor



VV: upwind  $\sim$  downwind  $>$  crosswind

HH: downwind  $\sim$  crosswind at the lowest grazing angle

Denoised NRCS is up to 10 dB lower than the noise floor

## Angular variation of the denoised NRCS: azimuthal variations

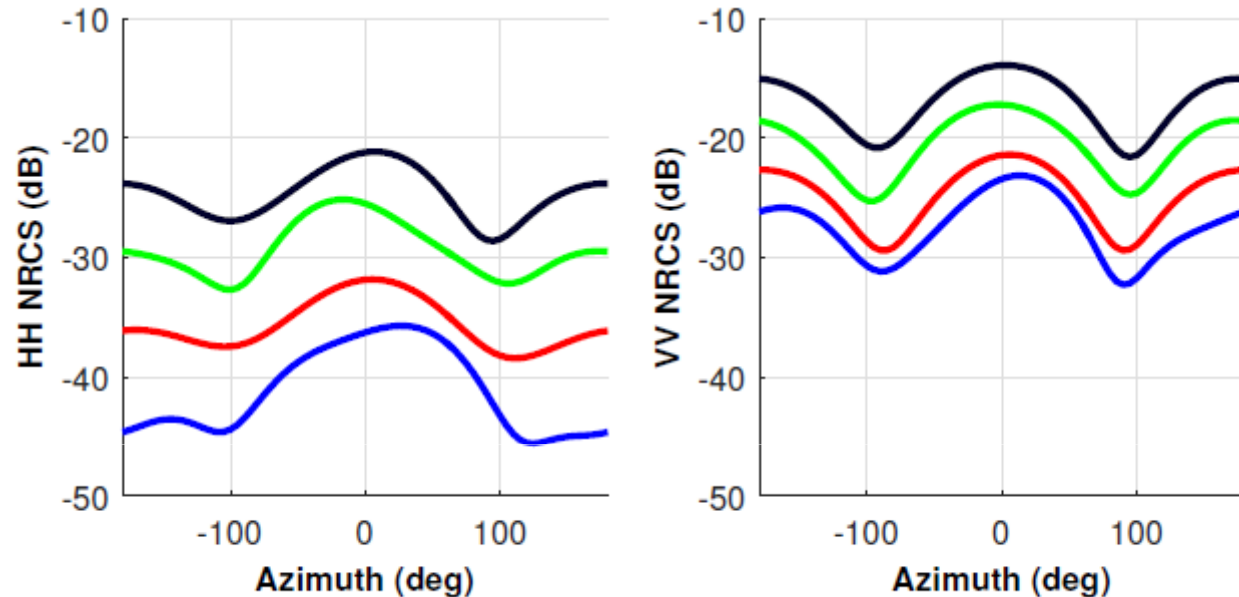
Run day 9

Grazing  $45^\circ$

Grazing  $35^\circ$

Grazing  $25^\circ$

Grazing  $16^\circ$



Moderate grazing angle: commonly observed pattern of a sinusoidal variation

As the grazing angle is decreased in HH pol, we observe a progressive shift from two local maxima at upwind and downwind directions to a unique and pronounced maximum in the upwind direction

=> physical modeling of this peculiar behavior is not established



# Model/data comparison

## Scattering models

- GOSSA [3] for the two-like polarizations
- SSA2 [4] for the cross-polarized data

## Spectral models

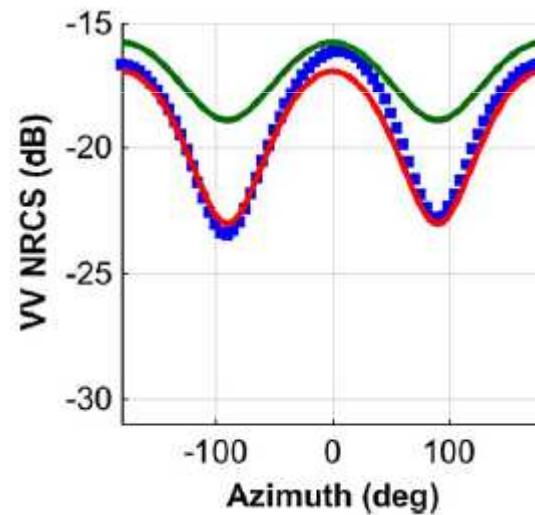
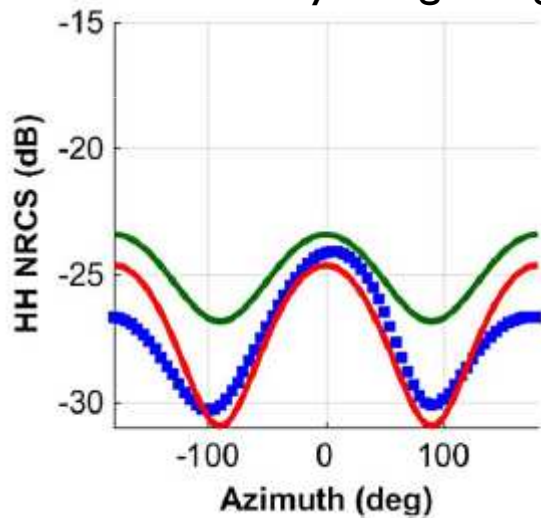
Omni-directional spectra

- Elfouhaily [5]
- Bringer [6]

spreading functions

- Elfouhaily [5]
- Yurovskaya [7]

Run day 9 – grazing 42°



■ INGARA  
— GOSSA+BY  
— GOSSA+Elf

Significant improvement brought by the use of the improved spectral models

[3] G. Soriano and C.A. Guérin, "A cutoff invariant two-scale model in electromagnetic scattering from sea surfaces," *Geoscience and Remote Sensing Letters*, IEEE, vol. 5, no. 2, pp. 199–203, 2008.

[4] C.-A. Guérin and J.-T. Johnson, "A simplified formulation for the crosspolarized backscattering coefficient under the second-order small slope approximation," *IEEE Trans. Geosci. and Remote Sens.*, 2015

[5] T. Elfouhaily and C.A. Guérin, "A critical survey of approximate scattering wave theories from random rough surfaces," *Waves in Random and Complex Media*, 2004.

[6] A. Bringer, B. Chapron, A. Mouche, and C.-A. Guérin, "Revisiting the short-wave spectrum of the sea surface in the light of the weighted curvature approximation," *IEEE Trans. Geosci. and Remote Sens.*, 2014.

[7] MV Yurovskaya, VA Dulov, Bertrand Chapron, and VN Kudryavtsev, "Directional short wind wave spectra derived from the sea surface photography," *Journal of Geophysical Research: Oceans*, 2013.

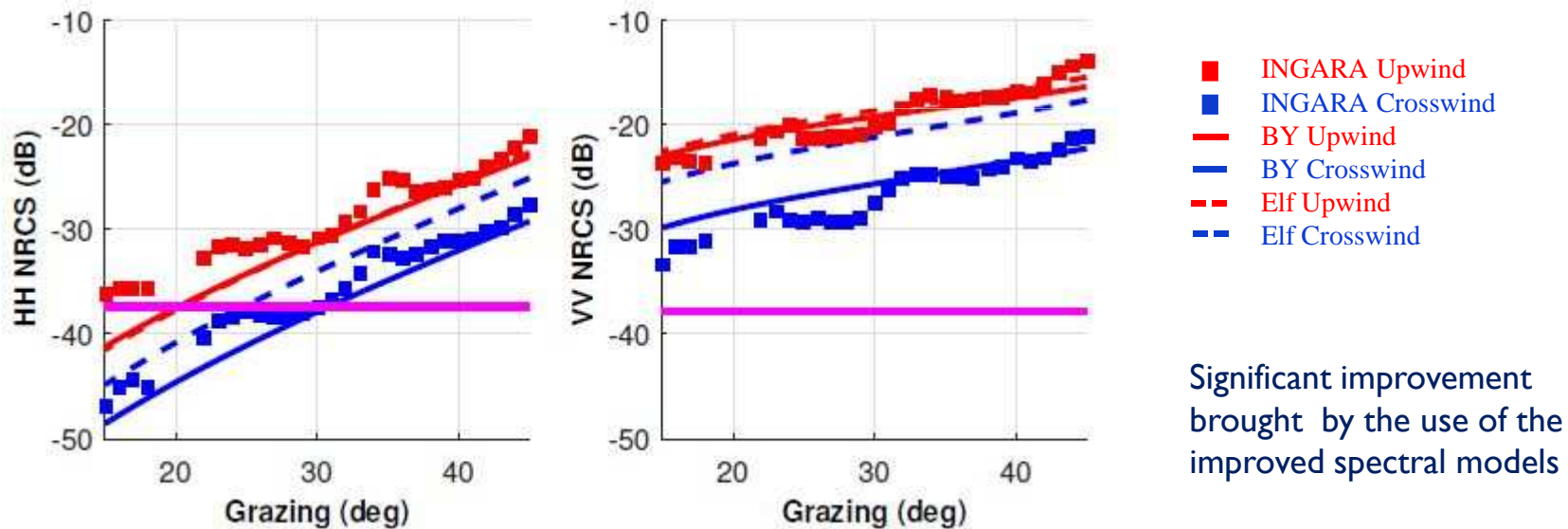
# Model/data comparison

## Scattering models

- GOSSA [3] for the two-like polarizations
- SSA2 [4] for the cross-polarized data

## Spectral models

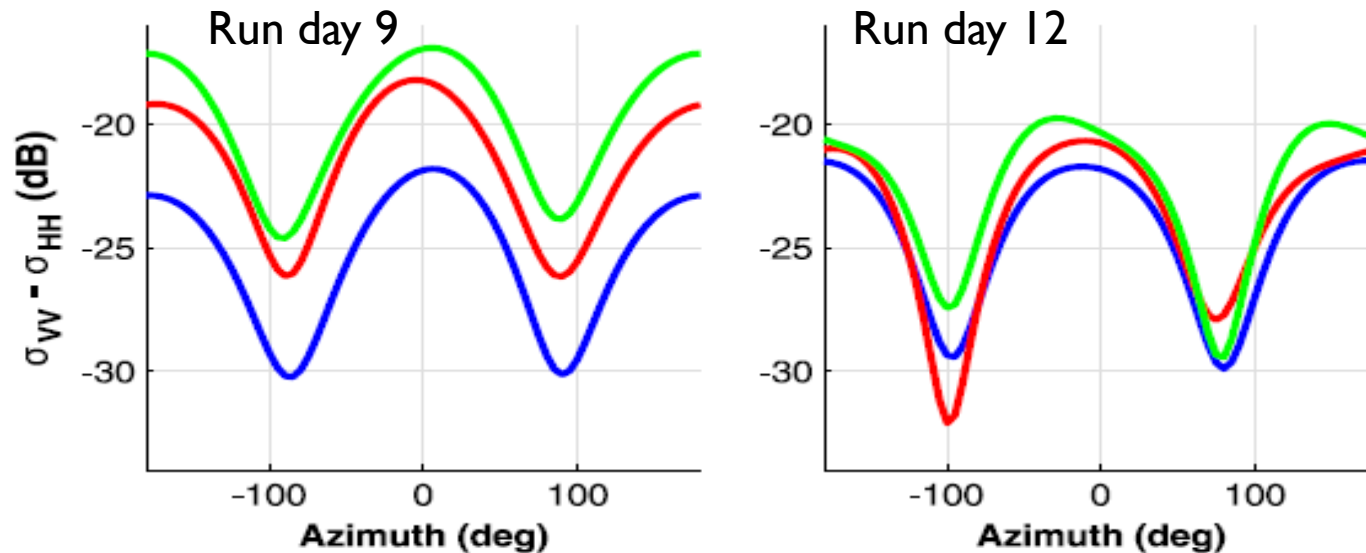
- |   |   |
|---|---|
| <ul style="list-style-type: none"> <li>• Omni-directional spectra</li> <li>• Elfouhaily [5]</li> <li>• Bringer [6]</li> </ul> | <ul style="list-style-type: none"> <li>• spreading functions</li> <li>• Elfouhaily [5]</li> <li>• Yurovskaya [7]</li> </ul> |
|---|---|



Significant improvement brought by the use of the improved spectral models

[3] G. Soriano and C.A. Guérin, "A cutoff invariant two-scale model in electromagnetic scattering from sea surfaces," *Geoscience and Remote Sensing Letters*, IEEE, vol. 5, no. 2, pp. 199–203, 2008.  
 [4] C.-A. Guérin and J.-T. Johnson, "A simplified formulation for the crosspolarized backscattering coefficient under the second-order small slope approximation," *IEEE Trans. Geosci. and Remote Sens.*, 2015  
 [5] T. Elfouhaily and C.A. Guérin, "A critical survey of approximate scattering wave theories from random rough surfaces," *Waves in Random and Complex Media*, 2004.  
 [6] A. Bringer, B. Chapron, A. Mouche, and C.-A. Guérin, "Revisiting the short-wave spectrum of the sea surface in the light of the weighted curvature approximation," *IEEE Trans. Geosci. and Remote Sens.*, 2014.  
 [7] MV Yurovskaya, VA Dulov, Bertrand Chapron, and VN Kudryavtsev, "Directional short wind wave spectra derived from the sea surface photography," *Journal of Geophysical Research: Oceans*, 2013.

## Relations between the different polarizations : *Polarization difference – Grazing and azimuth behavior*



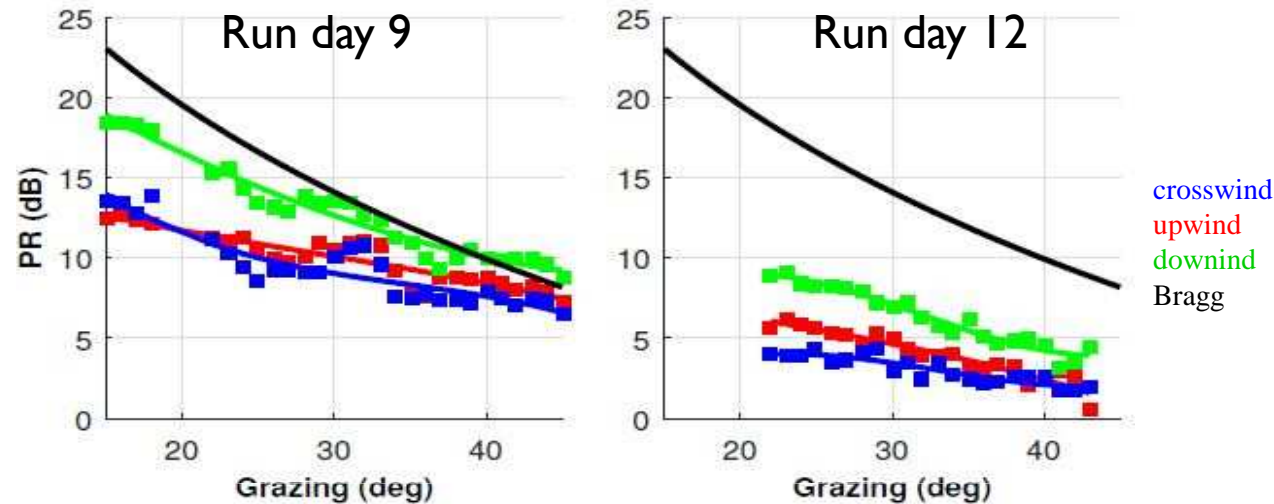
PD = VV – HH (linear unit)

PD is proportional to the wave number spectrum taken at the Bragg frequency, it is therefore more sensitive to the small scale features of the sea surface rather than the larger scale which are responsible for the unpolarized portion of the NRCS

PD doesn't exhibit the UDA asymmetry seen with the HH & VV pol

=> the UDA asymmetry is likely to be contained in the non-polarized part and presumably linked to the large scales of roughness

## Relations between the different polarizations : *Polarization ratio – Grazing and azimuth behavior*



$$PR = VV/HH$$

The PR is a decreasing function of grazing angle

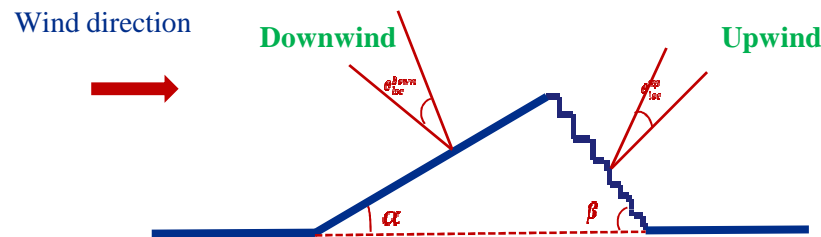
$$PR_{\text{experimental}} < PR_{\text{Bragg}}$$

PR has a strong azimuthal dependency with a sharp maximum in the downwind direction => **Can allow removing the usual ambiguity encountered between upwind and downwind directions**

# Polarization ratio of asymmetric wave profiles

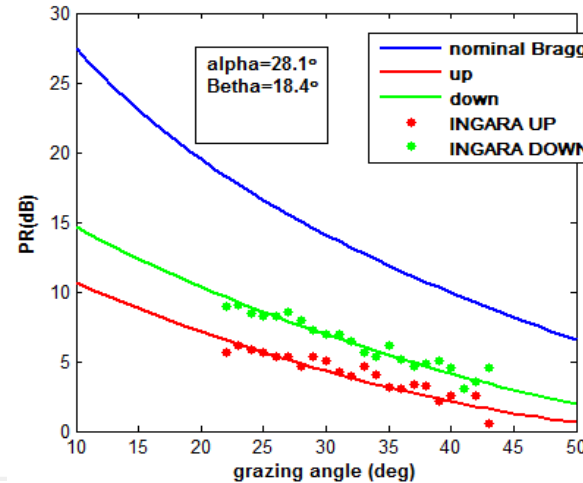
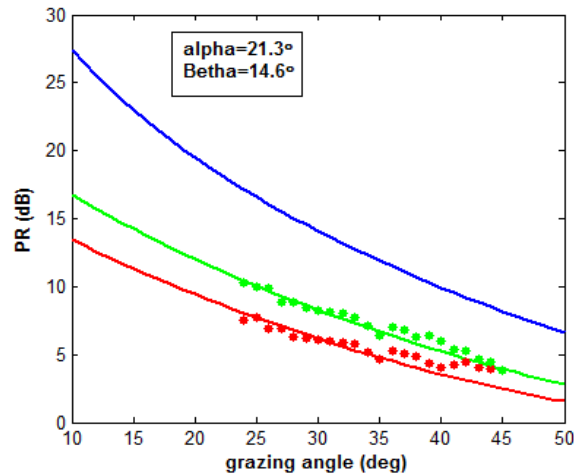
Polarization ratio using Bragg theory for a nominal incidence angle  $\theta$

$$PR_{Bragg} = \frac{|B_{VV}|^2}{|B_{HH}|^2} = f(\theta_{loc}, \varepsilon)$$



At local incidence angles:

$$PR_{loc} = PR(\theta_{loc}), \quad \theta_{loc} = \begin{cases} \theta_i - \alpha & \text{downwind} \\ \theta_i - \beta & \text{upwind} \end{cases}$$



$\alpha$  and  $\beta$  angles are in good agreement with slopes obtained in wind-wave tank measurements (Cf Caulliez et al <sup>(2)</sup>)

[2] Caulliez, G., and C.-A. Guerin (2012), Higher-order statistical analysis of short wind-waves, J. Geophys. Res., 117, C06002, doi:10.1029/2011JC007854.



# Study of the slope influence

- Based on Bragg theory, the slope influence is significantly more pronounced at **HH** than **VV** polarization.

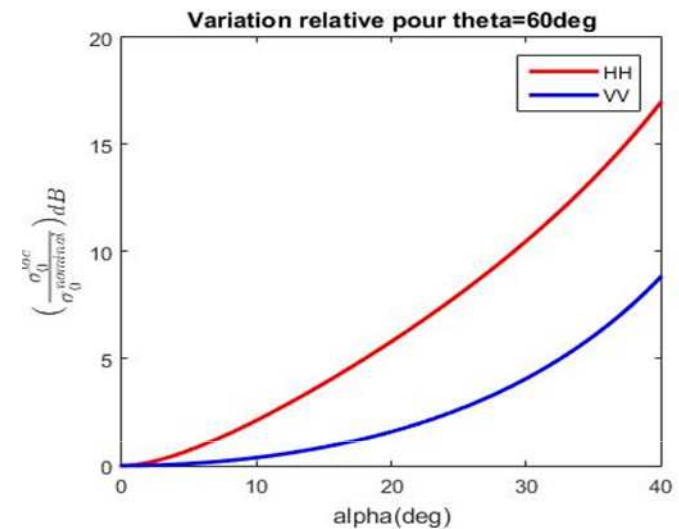
- Taylor expansion** with respect to the slope:

$$\begin{aligned}\sigma_{pp}^{0Bragg}(\theta_{loc}) &= \sigma_{pp}^{0Bragg}(\theta_i, \alpha) \\ &= \sigma_{pp}^{0Bragg}(\theta_i, 0) + \Delta\sigma_0^1(\theta_i) \alpha + \Delta\sigma_0^2(\theta_i) \frac{\alpha^2}{2} + \dots\end{aligned}$$

- Two scale-Model**

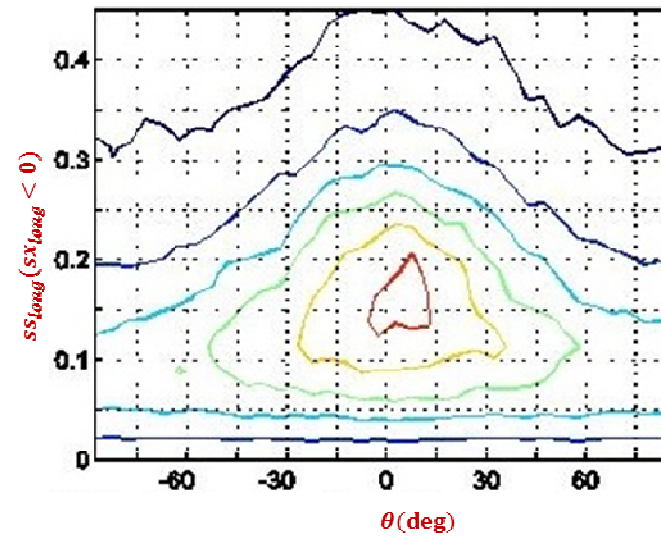
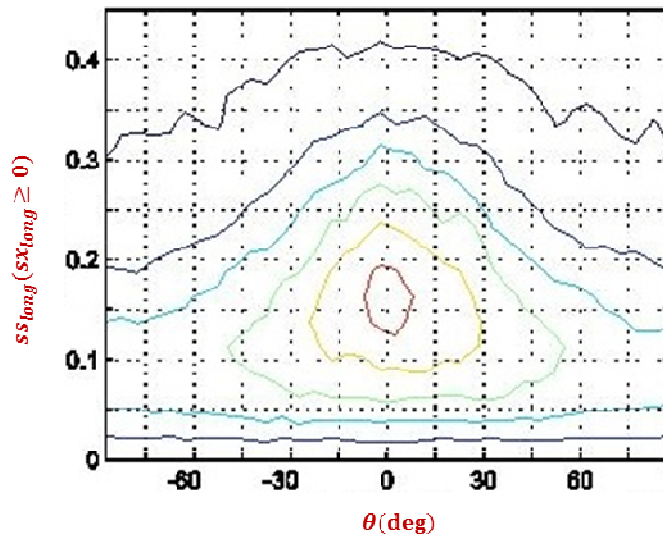
$$\begin{aligned}\bar{\sigma}_0(\theta_{loc}) &= \int_{-\infty}^{+\infty} p(\alpha) \sigma(\theta_i, \alpha) d\alpha \\ &= \sigma_{Bragg}(\theta_i, 0) + \underbrace{\Delta\sigma_0^1(\theta_i) \int_{-\infty}^{+\infty} \alpha p(\alpha) d\alpha}_{M_1} + \underbrace{\Delta\sigma_0^2(\theta_i) \int_{-\infty}^{+\infty} \alpha^2 p(\alpha) d\alpha}_{M_2}\end{aligned}$$

$$UDA = \frac{\sigma_{Bragg}(\theta_i, 0) + \Delta\sigma_0^1(\theta_i)M_1^+ + \Delta\sigma_0^2(\theta_i)M_2^+}{\sigma_{Bragg}(\theta_i, 0) + \Delta\sigma_0^1(\theta_i)M_1^- + \Delta\sigma_0^2(\theta_i)M_2^-}$$



# Study of the slope influence

Long waves (LF waves  $\lambda > 3cm$ ) –  $U = 8m/s$

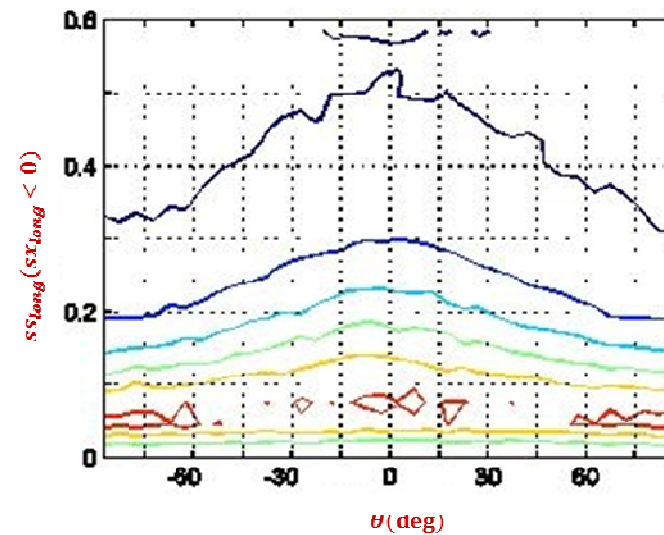
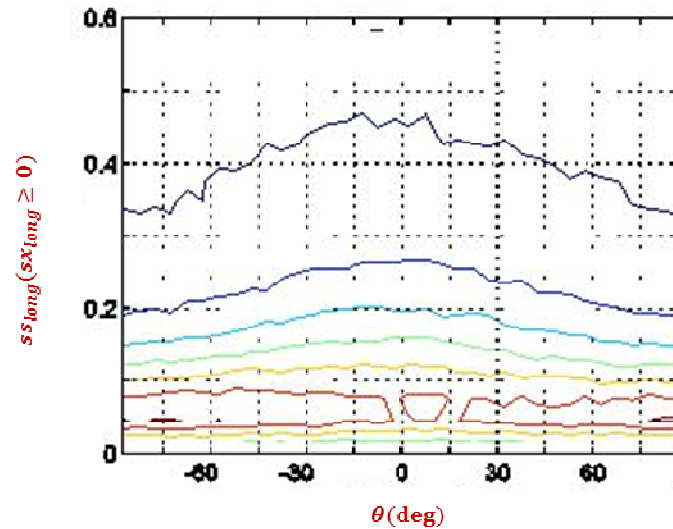


contours =  $1.10^{-8} * [0.1 \ 1 \ 2 \ 3 \ 4 \ 5 \ 6]$

- Anisotropic long waves: waves strongly aligned with the wind direction.
- Asymmetry of positive and negative slopes  $\rightarrow$  Asymmetric slope distribution.

# Study of the slope influence

Short waves ( HF waves  $\lambda \leq 3cm$ ) –  $U = 8m/s$



$$\text{contours} = 1.10^{-8} * [0.1 \ 1 \ 2 \ 3 \ 4 \ 5 \ 6]$$

- Isotropic short waves.
- Slight difference between positive and negative slopes.

# Conclusions & perspectives

## Conclusions

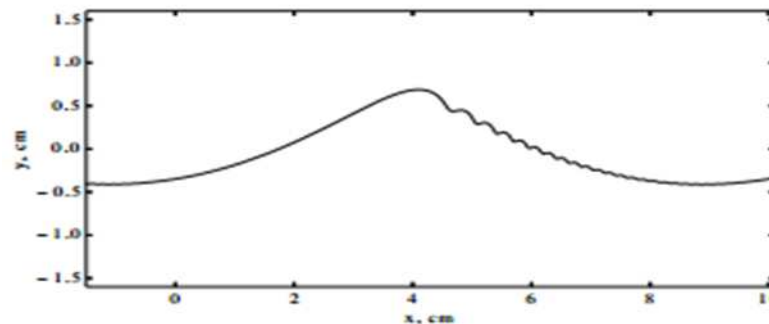
- Empirical/physical model for the azimuthal repartition of radar sea clutter.
- Study of the UDA, PD, PR and other parameters.
- Data/model comparison: Improvement of the co-polarized simulated NRCS brought by the use of improved spectral models.

Summerized in *Guerraou, Z.; Angelliaume, S.; Rosenberg, L.; Guerin, C.-A., "Investigation of azimuthal variations from X-band medium grazing angle sea clutter", IEEE TGRS*

- Evaluation of slope influence on the NRCS.

## Perspectives

- Quantification of the UDA using asymmetric slope distribution inferred from wave-trank measurements.
- Diffraction by non-linear wave fields including gravity-capillarity waves and their parasitic capillaries (Project in collaboration with V.Schira from the NOAA).



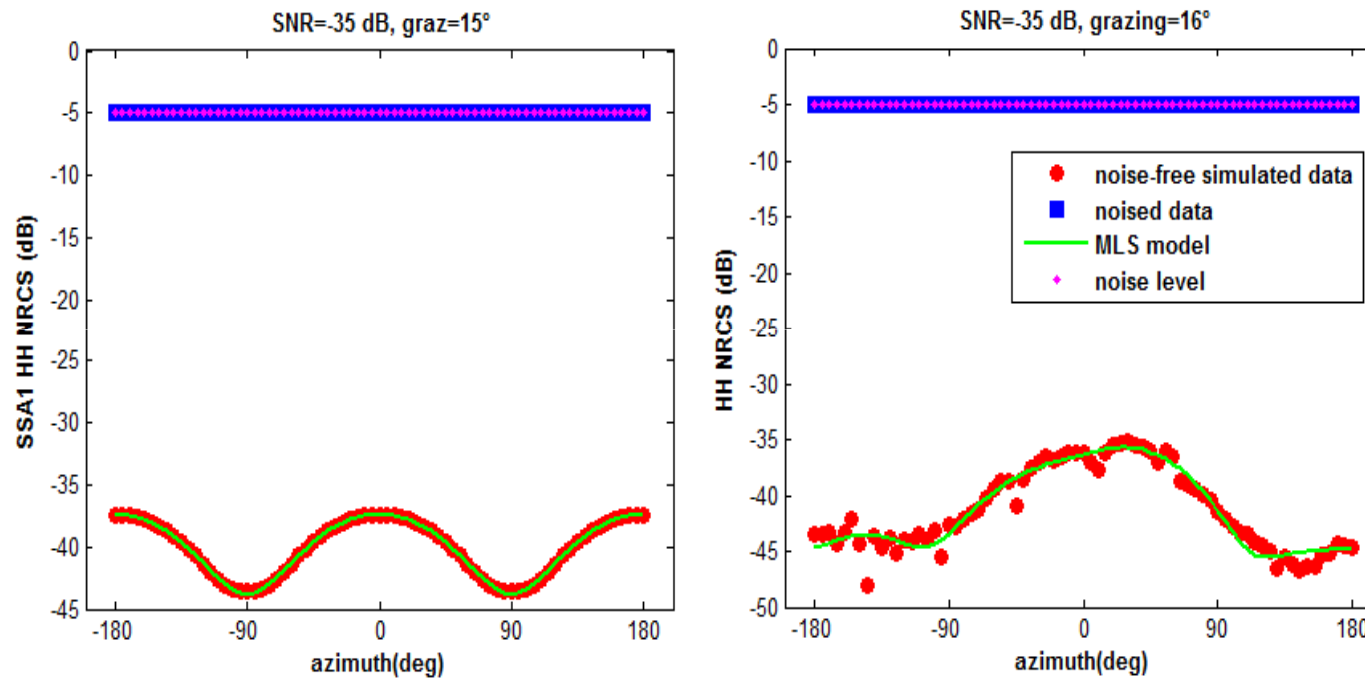
THANK YOU FOR YOUR  
ATTENTION

QUESTIONS?



# Azimuthal variation of the NRCS : Maximum Likelihood estimation

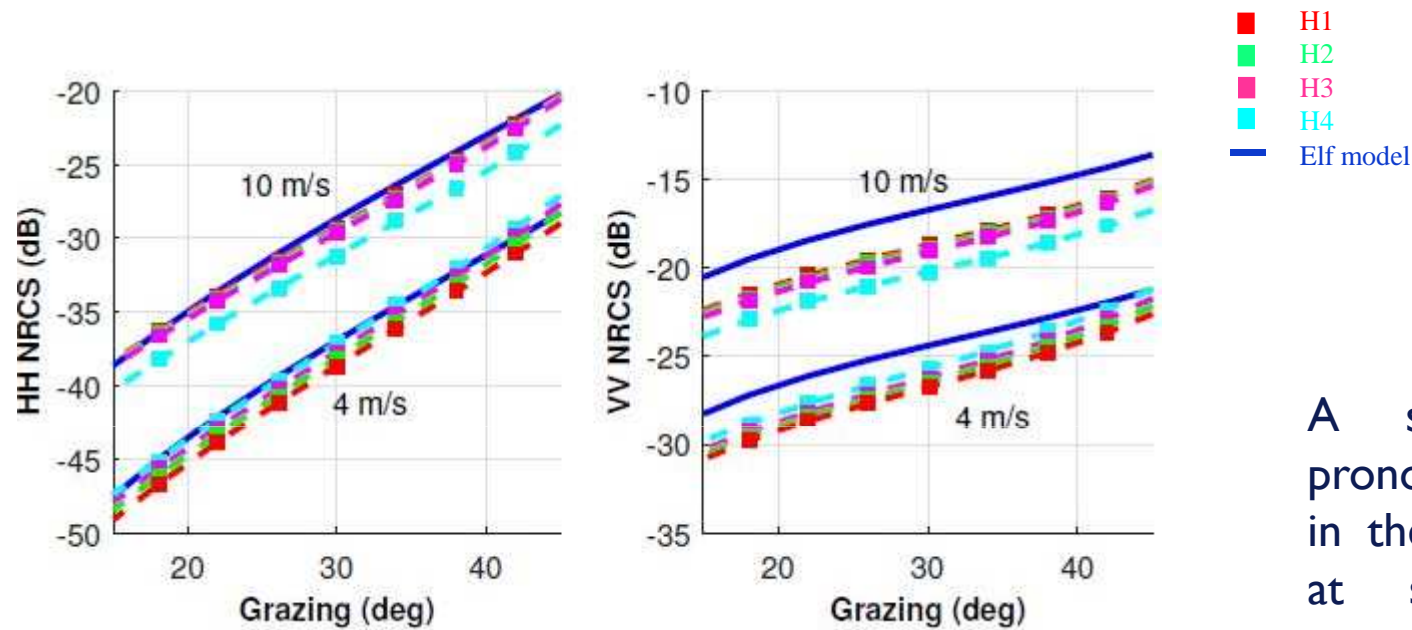
## Robustness of the MLE to the SNR degradation



The RMSE calculated between the noise-free simulated data and the estimated model is found to be significantly low and quite insensitive to the SNR.

*Example of NRCS reconstruction at low SNR of -35 dB*

# Effect of swell



A slightly more pronounced effect in the HH pol and at smaller wind speeds

VV(upper dots) and HH (lower dots) NRCS for the Hwang spectrum with different swell indices for a 4m/s wind speed on the left panel and 10m/s on the right panel